Current-limiting Droop Control with Virtual Inertia and Self-Synchronization Properties

Alexandros G. Paspatis and George C. Konstantopoulos

Dept. of Automatic Control and Systems Engineering
The University of Sheffield
Sheffield, S1 3JD, UK

Email: {apaspatis1, g.konstantopoulos}@sheffield.ac.uk

Abstract—In this paper a current-limiting droop control of grid-tied inverters that introduces virtual inertia and operates without a phase locked loop unit is proposed. The proposed controller inherits a self-synchronization function and can guarantee tight bounds for the inverter frequency. In addition, using nonlinear Lyapunov theory, it is analytically proven that the inverter current never violates a given maximum value. Compared to the original current-limiting droop controller, the maximum capacity of the inverter is utilized at all times using the proposed strategy, even under grid faults. It is also proven that the proposed controller significantly reduces the resonance problem of the LCL filter. Extended simulation results are presented to verify the performance of the proposed controller under normal and faulty grid conditions.

I. Introduction

The increased penetration of distributed energy resources (DERs) in the main power grid or into smaller power networks, i.e. microgrids, has raised concerns with regard to power system stability, reliability and protection [1]. To this end, a variety of control methods have been applied in order to support the resilience of power systems dominated by DERs, with most commonly used techniques being the PQ set control, I/V control, droop control and secondary control methods [2].

Droop control is a widely used technique for inverter-interfaced DERs. In particular, by familiarizing the DERs control system with the conventional techniques used for synchronous generators, the control system can adjust the voltage and the frequency at the connection point according to load changes, faults, disturbances or structural changes that may occur in the power grid [3], [4], [5]. However, opposed to conventional synchronous generators, droop-controlled inverters do not introduce inertia leading to increased frequency fluctuations. Virtual inertia can be introduced via the control design and when combined with droop control, it can mimic the transient response of a synchronous generator [6], such as the case of the virtual synchronous generator (VSG) [7], [8], the virtual synchronous machine (VISMA) [9] and the synchronverter [10]. A comparison between VSG and droop control can be found in [11].

Furthermore, as it has been pointed out in [12], there is a resemblance between the structure of the droop control and the phase-locked-loop (PLL), which has been believed to be an indispensable device for inverters to synchronize with the grid. This has motivated researchers to design self-synchronization

methods as part of the controller of inverter-interfaced DERs [13], [14], [15]. The main reasons for removing the PLL is that PLLs are inherently nonlinear and they can degrade the response time and accuracy of the pre-synchronization process [16]. In addition, in [17], it is shown that under large grid impedances, the control system can be driven to instability due to the interaction between the PLL and the current controller. Hence control methods such as the self-synchronized synchronverter have been successfully implemented in grid-tied inverters to increase system reliability [18].

Although droop controlled inverters with or without self-synchronization can support the grid voltage and frequency regulation under normal grid conditions, in the case of grid faults, the inverter current increases and droop control is changed to a different current-limiting control strategy [19]. In practice, the currents injected to the grid should not exceed specific limits defined by the converter and grid characteristics [20]. Since the use of current saturation and switching between droop control and current-limiting control can lead to integrator windup and instability [20], a droop controller with inherent current-limiting capability has been proposed in [21] to overcome these issues. However, this current-limiting droop (CLD) controller cannot utilize the maximum capacity of the inverter during grid faults since the current is limited to a lower value depending on the voltage sag. Furthermore, the CLD does not introduce any inertia and it requires a PLL for its implementation which, as mentioned above, decreases the system reliability.

In this paper, a novel enhanced version of the CLD controller for grid-tied inverters is proposed that: i) guarantees a current limitation below a maximum value at all times, even during faults, by fully utilizing the capacity of the inverter, ii) introduces a virtual inertia to the system and iii) inherits a self-synchronization property without the need of a PLL. Motivated by the recently developed self-synchronization methods, this new CLD structure can remove the PLL and offer a simple transition between droop control mode and accurate real and reactive power regulation mode. Additionally, the proposed structure inherits the bounded integral controller [22] in order to guarantee tight bounds for the inverter frequency, as required by the Grid Code. Furthermore, based on nonlinear input-to-state stability theory, the current-limiting property of the

proposed controller is mathematically proven to be sustained at all times. Finally, the effect of the LCL output filter to the closed loop system is also investigated. Extended simulation results of a single-phase grid-tied inverter under both normal grid and grid voltage sags are presented to validate the desired performance of the proposed control strategy.

The paper is organized as follows. In Section II, the research problem is stated. In Section III, the proposed control strategy is presented and analyzed, and the current-limiting property is analytically proven. In Section IV, the effect that the LCL output filter has to the closed loop system is investigated and in Section V, practical implementation issues are discussed. In Section VI, simulation results are presented and in Section VII, the conclusions derived from this work are given.

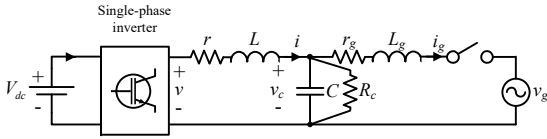## II. PROBLEM FORMULATION

Figure 1. The inverter connected to the grid via an LCL filter

Consider the system of an inverter with an LCL filter connected to the grid as depicted in Fig. 1. The dynamic equations of this system can be obtained as

$$L\frac{di}{dt} = -ri + v - v_c$$
$$C\frac{dv_c}{dt} = i - \frac{v_c}{R_C} - i_g \qquad (1)$$
$$L_g\frac{di_g}{dt} = v_c - r_g i_g - v_g.$$

The filter and grid inductances are denoted as L and L_g in series with the small parasitic resistances r and r_g, respectively, while the filter capacitance is C with a large parasitic resistance R_c in parallel. The output voltage and current of the inverter are v and i, respectively, the grid voltage is v_g and the control input is represented by the inverter voltage v.

Droop control is the most commonly used control technique for inverters to support the grid voltage and frequency regulation. The traditional droop control equations are

$$\omega = \omega_n - m\left(P - P_{set}\right)$$
$$E = E^* - n\left(Q - Q_{set}\right)$$

where ω is the inverter angular frequency, E is the RMS inverter voltage, ω_n is the nominal angular frequency, E^* is the nominal output voltage, P, Q are the output real and reactive power values and P_{set}, Q_{set} correspond to the reference power values. Finally, m and n are the droop coefficients.

Depending on the application or the desired operation of the control system, several modifications have been proposed to the conventional droop control scheme. A lot of these works emphasize on the output impedance of the inverter and can be modified using virtual impedance methods. In these cases, the droop equations are modified to $P \sim E$ and $Q \sim -\omega$, when the impedance is resistive or $P \sim -\omega$ and $Q \sim -E$, when the impedance is capacitive [23], [24], [25]. The universal droop controller [25] which does not depend on the type of output impedance take the form

$$\omega = \omega_n + m\left(Q - Q_{set}\right) \qquad (2)$$
$$\dot{E} = K_e(E^* - V_c) - n\left(P - P_{set}\right) \qquad (3)$$

and will be adopted in this paper. Note that K_e is a positive gain and V_c is the RMS output voltage.

The droop control structure (2)-(3) has been used in the CLD [21] in order to support the grid and additionally limit the inverter current in the cases of grid faults. However, a drawback of the CLD is that the current is limited to a lower value that depends on the grid voltage sag, thus not fully utilizing the capacity of the inverter. Additionally, it requires a PLL for the implementation and does not introduce any inertia to the system. A control method that overcomes all of these issues is proposed in the sequel.

III. METHODOLOGY

A. The proposed controller

In Fig. 2, the proposed self-synchronized current-limiting droop controller for the grid-connected inverter shown in Fig. 1, is being displayed. The proposed controller has the ability to utilize the maximum capacity of the inverter and takes the form

$$v = v_c + (1 - w_q^l)(\sqrt{2}E^* \sin\theta - wi), \qquad (4)$$

where $l \geqslant 1 \in \mathcal{N}$ and w represents a dynamic virtual resistance which together with the controller state w_q, is given as

$$\dot{w} = -c_w f(P, V_C) w_q^2 \qquad (5)$$
$$\dot{w}_q = \frac{c_w(w - w_m)w_q}{\Delta w_m^2} f(P, V_c) - k_w \left(\frac{(w - w_m)^2}{\Delta w_m^2} + w_q^2 - 1\right) w_q \qquad (6)$$

with

$$f(P, V_c) = n(P_{set} - P) + K_e(E^* - V_c). \qquad (7)$$

Here $w_m, \Delta w_m, c_w, k_w$ are positive constants with $w_m > \Delta w_m$.

The w, w_q dynamics introduce the $P \sim V$ droop function and similar to the analysis of the original CLD in [21], for initial conditions $w = w_m$ and $w_{q0} = 1$, there is $w \in [w_{min}, w_{max}] = [w_m - \Delta w_m, w_m + \Delta w_m] > 0$ and $w_q \in [0, 1]$ for all $t \geqslant 0$.

For the calculation of the phase θ in (4), and consequently the frequency ω, a self-synchronization mechanism is adopted using a PI controller as shown in Fig. 2, motivated by the self-synchronized synchronverter [18]. However, since the frequency $f = \frac{\omega}{2\pi}$ is required to remain in a bounded range, eg. [49.5, 50.5] Hz, in this paper the bounded integral controller
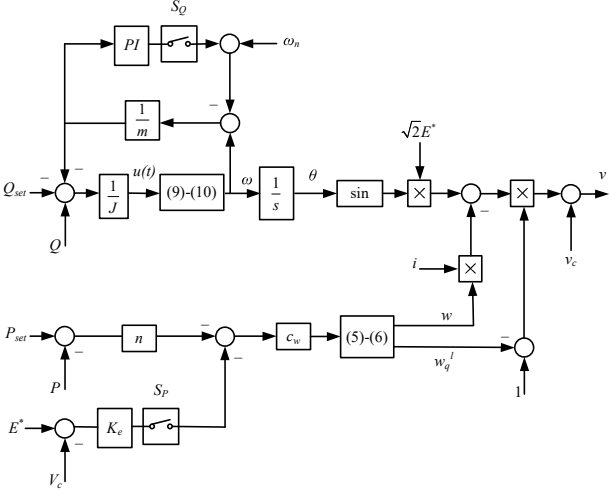
Figure 2. The proposed controller

(BIC) of [22] is used to replace the traditional integrator in the frequency dynamics. Since the BIC guarantees a bound for the frequency without any saturation units, it prevents wind up phenomena and instability in the frequency dynamics. Thus, the frequency dynamics take the form

$$\dot{\theta} = \omega \qquad (8)$$

$$\dot{\omega} = u(t)\omega_q^2 \qquad (9)$$

$$\dot{\omega}_q = -\frac{(\omega - \omega_n)\omega_q}{\Delta\omega_m^2}u(t) - k_\omega\left(\frac{(\omega - \omega_n)^2}{\Delta\omega_m^2} + \omega_q^2 - 1\right)\omega_q \quad (10)$$

where $u(t)$ results from the inverse Laplace transformation of

$$u(s) = \frac{1}{J}\left(Q(s) - Q_{set} - \frac{1}{m}(\omega(s) - \omega_n - \omega_{PI}(s))\right),$$

with

$$\omega_{PI}(s) = \frac{(K_P s + K_I)(\omega(s) - \omega_n)}{(m + K_P)s + K_I},$$

when S_Q is closed. Parameter k_w is a positive constant and $K_P, K_I > 0$ represent the proportional and integral gain of the PI controller. Additionally, $\Delta\omega_m$ is the maximum acceptable frequency derivation from the nominal value. For example, for a nominal frequency of 50 Hz with maximum deviation 0.5 Hz, there is $\omega_n = 100\pi$ rad/s and $\Delta\omega_m = \pi$ rad/s.

A significant difference that distinguishes the proposed controller with the original CLD [21] is the self-synchronization property in the frequency dynamics for the calculation of the phase θ, opposed to the original CLD which used a traditional PLL. A second key difference is the use of the nominal voltage E^* in (4) instead of the grid voltage V_g. The original CLD fails to utilize the maximum capacity of the inverter under faults, i.e. the inverter current is limited to a lower value depending on the grid voltage drop, which is a significant disadvantage in grid-connected units to support the grid under faulty conditions. The difference in the structure of (4) enables the current-limiting property with maximum capacity utilization as shown below.

B. Current-limiting property

By applying the proposed controller (4) into the grid-tied inverter dynamics (1), the dynamics of the inverter current take the form

$$L\frac{di}{dt} = -(r + (1 - w_q^l)w)i + (1 - w_q^l)\sqrt{2}E^*\sin\theta. \quad (11)$$

Following the analysis of the original CLD dynamics for w and w_q, it holds true (for details see [21]) that $w \in [w_{min}, w_{max}] > 0$, where $w_{min} = w_m - \Delta w_m$, $w_{max} = w_m + \Delta w_m$, and $w_q \in [0, 1]$ for all $t \geq 0$. For system (11), let us consider the Lyapunov function candidate

$$V = \frac{1}{2}Li^2, \qquad (12)$$

which actually represents the energy stored in the inductor L. Therefore, the time derivative of V becomes

$$\dot{V} = -(r + (1 - w_q^l)w)i^2 + (1 - w_q^l)\sqrt{2}E^*i\sin\theta$$
$$\leq -(r + (1 - w_q^l)w_{min})i^2 + (1 - w_q^l)\sqrt{2}E^*|i||\sin\theta|.$$

This shows that $\dot{V} < 0$ when $|i| > \frac{(1 - w_q^l)\sqrt{2}E^*|\sin\theta|}{r + (1 - w_q^l)w_{min}}$, proving that (11) is input-to-state stable (ISS) assuming as input the expression $(1 - w_q^l)\sqrt{2}E^*\sin\theta$. Since this expression is bounded, then the inverter current i is bounded for all $t \geq 0$. According to the ISS property, it holds true that

$$|i| \leq \frac{(1 - w_q^l)\sqrt{2}E^*}{r + (1 - w_q^l)w_{min}}, \forall t \geq 0,$$

if initially $i(0)$ satisfies the previous inequality. Since w_{min} is one of the controller parameters ($w_{min} = w_m - \Delta w_m$), by selecting

$$w_{min} = \frac{E^*}{I_{max}} \qquad (13)$$

where I_{max} is the maximum allowed RMS value of the inverter current, then

$$|i| \leq \frac{(1 - w_q^l)}{r\frac{I_{max}}{E^*} + (1 - w_q^l)}\sqrt{2}I_{max} < \sqrt{2}I_{max}, \quad (14)$$

since $(1 - w_q^l) \geq 0$ and $r\frac{I_{max}}{E^*} > 0$. The previous inequality holds for any $t \geq 0$ and for any constant positive I_{max}. As a result

$$I < I_{max}, \forall t \geq 0, \qquad (15)$$

where I is the RMS value of the inverter current, showing that the proposed controller maintains the current-limiting property below a given value I_{max}. Since the closed-loop current equation (11) does not depend on the grid voltage v_g, then the current-limiting property holds independently from any grid voltage variations, eg. grid faults.
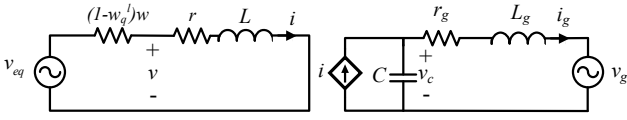
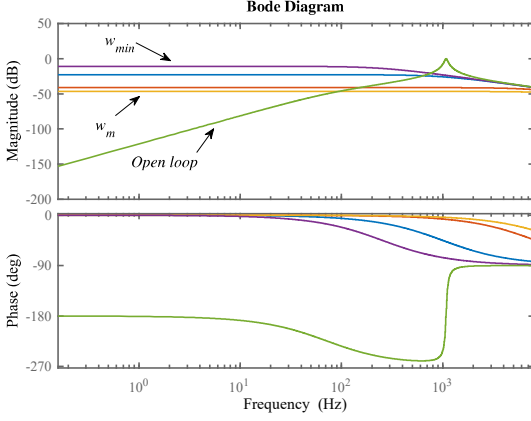Figure 3. Equivalent circuit of the closed-loop system

Figure 4. Bode diagram of $\frac{i(s)}{v_{eq}(s)}$ for $w \in [w_{min}, w_m]$

IV. EFFECT OF THE LCL FILTER TO THE CLOSED-LOOP SYSTEM

LCL filters are widely used in inverter-interfaced sources due to their ability to reduce the harmonic content resulting from the pulse width modulation. However, the main drawback of these topologies is the high gain that they introduce at the resonance frequency [26]. Depending on the controller structure and dynamics the closed-loop system may become unstable due to this resonance issue. In order to realize the effect of the LCL to the closed-loop system based on the proposed controller, the closed loop system resulting from the combination of (1) and (4) with dynamics (5)-(10) is inves-
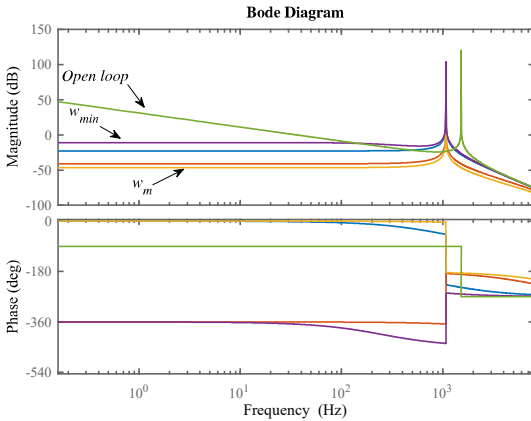

Figure 5. Bode diagram of $\frac{i_g(s)}{v_{eq}(s)}$ for $w \in [w_{min}, w_m]$

tigated. By replacing (4) into (1) the equivalent closed loop circuit is shown in Fig. 3 where $v_{eq} = (1 - w_q^l)\sqrt{2}E^* \sin \theta$. Hence, the transfer functions from the voltage $v_{eq}(s)$ to the inverter current $i(s)$ and to the grid current $i_g(s)$ are

$$\frac{i(s)}{v_{eq}(s)} = \frac{1}{Ls + r + (1 - w_q^l)w} \tag{16}$$

and

$$\frac{i_g(s)}{v_{eq}(s)} = 1/\left[LL_gCs^3 + (r_gCL + L_gCr + L_gC(1 - w_q^l)w)s^2 + \tag{17}\right.$$

$$\left. + (L + rr_gC + r_gC(1 - w_q^l)w)s + r + (1 - w_q^l)w \right].$$

Since the values of w and w_q change during the inverter operation but remain bounded in a given range, both (16) and (17) represent a set of transfer functions. Given that w starts from the initial condition $w_o = w_m$ and can reach the minimum value w_{min} at the maximum current, then the bode diagrams of (16) and (17) are provided in Fig. 4 and Fig. 5, respectively, for $w \in [w_{min}, w_m] = [w_m - \Delta w_m, w_m]$ and by neglecting r, r_g. Since from (6), w_q is restricted on the ellipse $\frac{(w - w_m)^2}{\Delta w_m^2} + w_q^2 = 1$ and $w_q \in [0, 1]$, then $w_q = \sqrt{1 - \frac{(w - w_m)^2}{\Delta w_m^2}}$ [21]. In the same figure, the open-loop transfer functions for an LCL filter are provided. Note that the parameters of Table I have been taken into account. In Fig. 4, it is observed that considering the proposed controller dynamics, the resonance of the LCL filter is avoided. However, in Fig. 5, for the transfer function $\frac{i_g(s)}{v_{eq}(s)}$, one can see that the resonance still exists with the proposed controller but with a limited value. Nevertheless, since the BIC is adopted in the proposed controller, the frequency of v_{eq} is bounded between 49.5 Hz and 50.5 Hz. Hence, the operation of the system remains away from the resonance depicted in higher frequencies and shows that every grid-tied inverter equipped with the proposed control strategy will never suffer from resonance issues.

V. PRACTICAL IMPLEMENTATION

In typical grid-connected inverter applications the values of L_g and r_g are often small, and both the phase shift and the voltage drop across the inductor can be ignored, resulting in $v_g \approx v_c$. Hence, the output voltage v_c used in (4) can be considered as equal to the grid voltage v_g, and the proposed controller can take the form

$$v = v_g + (1 - w_q^l)(\sqrt{2}E^* \sin \theta - wi). \tag{18}$$

This expression is also suitable for the initial connection of the inverter with the grid since according to the initial condition of the controller state $w_{q0} = 1$, then $v = v_g$ before the connection. Hence, a smooth connection can be achieved. After connecting with the grid, the controller can be enabled at any time with no need of a pre-connection synchronization.

Furthermore, different operating modes of the inverter can result from the state of the switches S_Q and S_P. When S_Q is closed, the Q-set mode is enabled which means that the

Table I
SYSTEM AND CONTROLLER PARAMETERS

Parameters	Values	Parameters	Values
L, L_g	2.2 mH	ω_n	2π x 50 rad/s
r, r_g	0.5 Ω	ω_g	2π x 49.98 rad/s
C	10 μF	I_{max}	8 A
$V_g = E^*$	110 V	l	100
J	$0.001 kg.m^2$	w_m	318.25 Ω
S_n	880 VA	Δw_m	304.5 Ω
c_w	348	K_e	10
k_w	1000	k_ω	1000
n	0.0625	m	0.0036
K_P	0.1	K_I	1
$\Delta\omega_m$	π rad/s	t_s	0.05 s

output reactive power can be regulated to its reference value. When this switch is opened, the Q-droop mode is enabled and the output reactive power results from the droop equation according to the frequency regulation. For the real power, when S_P is closed, the P-droop mode is enabled and when it opens, the P-set mode is activated. In this way, a simple and easy change of the inverter operating mode can be accomplished by the proposed controller.

VI. SIMULATION RESULTS

In order to verify the effectiveness of the proposed controller a single-phase grid-connected inverter is simulated under both normal and faulty grid conditions. The parameters of the power and the control systems used for the simulations, are depicted in Table I. The scenario is as follows: The inverter is connected to the grid at 0.1 s. Initially, the P-set and Q-set control is enabled by setting the desired values of the real and reactive power. Initially, the real power reference is set to 100 W and after 2 s changes to 500 W, while the reactive power is set to 0 Var and at 3 s changes to 50 Var, as shown in Fig. 6a and Fig. 6b. It is observed that both the real and the reactive power are regulated to their reference values after a short transient. At 4 s the droop control for both the real and the reactive power, is enabled and the real and reactive power injected to the grid change according to the droop expressions as shown in Fig. 6a and 6b. At 7 s, a voltage drop of 0.3 p.u. occurs and lasts for 2.5 s in order to investigate a grid fault. Under this grid fault, the injected power to the grid remains limited (Fig. 6a and Fig. 6b) because as shown in Fig. 6d, the current-limiting property of the proposed controller maintains the RMS current under the maximum value. When the fault is self-cleared, both the real and the reactive power return to their original values. In Fig. 7a, the response of the controller state w is depicted and in Fig. 7b a comparison between the inverter frequency that is obtained via the self-synchronization process of the proposed controller and the grid frequency measured from a conventional PLL is illustrated. One can observe that the inverter equipped with the proposed self-synchronized CLD remains synchronized with the grid at all times and that the inverter frequency stays always inside the desired range [49.5 Hz, 50.5 Hz], even during faults in the grid voltage. It should be noted that the conventional

(a) Real power

(b) Reactive power

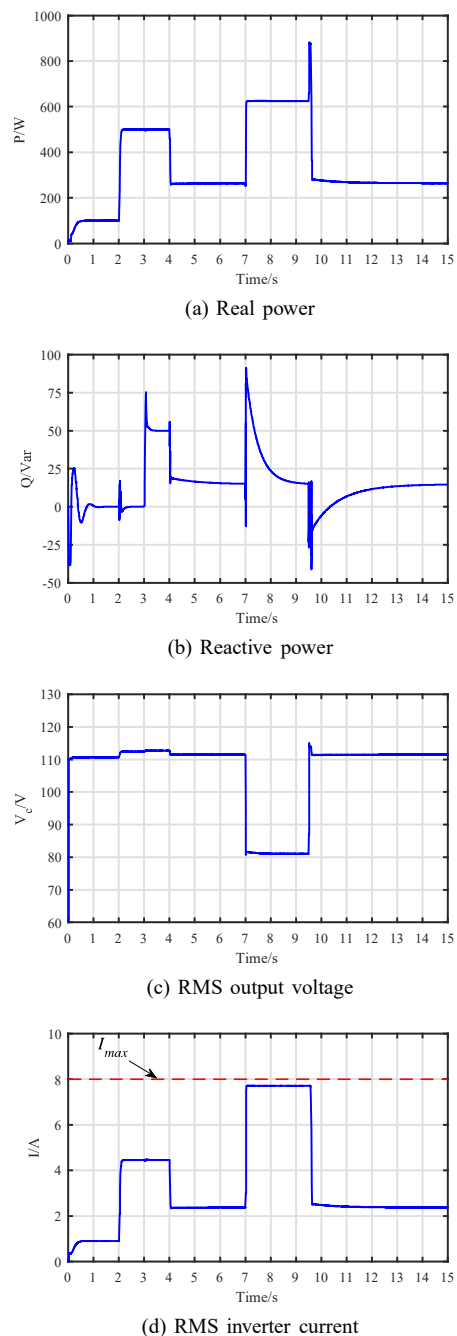(c) RMS output voltage

(d) RMS inverter current

Figure 6. Simulations results of a grid-tied inverter operating under the proposed self-synchronized CLD controller

PLL is used only for comparison purposes and is not part of the proposed controller.

VII. CONCLUSIONS

A novel droop controller without a PLL which introduces virtual inertia and current-limiting properties for grid-tied inverters was presented in this paper. It was analytically proven that the maximum capability of the inverter can be utilized during faults, i.e. during a sudden grid voltage dip, and at the same time the proposed controller maintains the current

(a) Controller state w

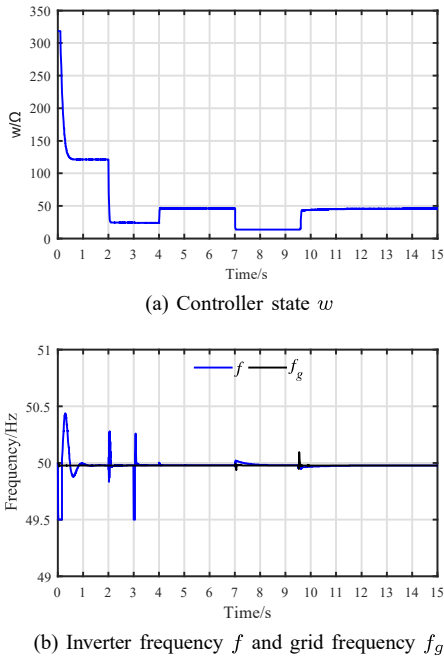(b) Inverter frequency f and grid frequency f_g

Figure 7. Time response of the proposed self-synchronized CLD dynamics

under a given maximum value. Extensive simulation results were presented to verify the proposed control approach.

REFERENCES

[1] M. H. Bollen and F. Hassan, *Integration of Distributed Generation in the Power System.* Wiley, 2011.

[2] D. E. Olivares, A. Mehrizi-Sani, A. H. Etemadi, C. A. Canizares, R. Iravani, M. Kazerani, A. H. Hajimiragha, O. Gomis-Bellmunt, M. Saeedifard, R. Palma-Behnke, G. A. Jimenez-Estevez, and N. D. Hatziargyriou, "Trends in microgrid control," *IEEE Transactions on Smart Grid*, vol. 5, no. 4, pp. 1905–1919, July 2014.

[3] M. Chandorkar, D. Divan, and R. Adapa, "Control of parallel connected inverters in standalone ac supply systems," *IEEE Transactions on Industry Applications*, vol. 29, no. 1, pp. 136–143, Jan. 1993.

[4] G. Diaz, C. Gonzalez-Moran, J. Gomez-Aleixandre, and A. Diez, "Scheduling of droop coefficients for frequency and voltage regulation in isolated microgrids," *IEEE Transactions on Power Systems*, vol. 25, no. 1, pp. 489–496, Feb 2010.

[5] J. Liu, Y. Miura, and T. Ise, "Comparison of dynamic characteristics between virtual synchronous generator and droop control in inverter-based distributed generators," *IEEE Trans. Power Electron.*, vol. 31, no. 5, pp. 3600–3611, 2016.

[6] X. Hou, H. Han, C. Zhong, W. Yuan, M. Yi, and Y. Chen, "Improvement of transient stability in inverter-based ac microgrid via adaptive virtual inertia," in *2016 IEEE Energy Conversion Congress and Exposition (ECCE)*, Sept 2016, pp. 1–6.

[7] J. Driesen and K. Visscher, "Virtual synchronous generators," in *2008 IEEE Power and Energy Society General Meeting - Conversion and Delivery of Electrical Energy in the 21st Century*, July 2008, pp. 1–3.

[8] V. Karapanos, S. de Haan, and K. Zwetsloot, "Real time simulation of a power system with vsg hardware in the loop," in *IECON 2011 - 37th Annual Conference of the IEEE Industrial Electronics Society*, Nov 2011, pp. 3748–3754.

[9] J. A. Martinez and J. Martin-Arnedo, "Impact of distributed generation on distribution protection and power quality," in *2009 IEEE Power Energy Society General Meeting*, July 2009, pp. 1–6.

[10] Q.-C. Zhong and T. Hornik, *Synchronverters: Grid-Friendly Inverters That Mimic Synchronous Generators.* Wiley-IEEE Press, 2012, pp. 277–296.

[11] J. Liu, Y. Miura, and T. Ise, "Comparison of dynamic characteristics between virtual synchronous generator and droop control in inverter-based distributed generators," *IEEE Transactions on Power Electronics*, vol. 31, no. 5, pp. 3600–3611, May 2016.

[12] Q.-C. Zhong and D. Boroyevich, "A droop controller is intrinsically a phase-locked loop," in *Proc. of the 39th Annual Conference of the IEEE Industrial Electronics Society, IECON 2013*, Vienna, Austria, Nov. 2013, pp. 5916–5921.

[13] T. Younis, M. Ismeil, E. K. Hussain, and M. Orabi, "Single-phase self-synchronized synchronverter with current-limiting capability," in *2016 Eighteenth International Middle East Power Systems Conference (MEPCON)*, Dec 2016, pp. 848–853.

[14] M. Ashabani, F. D. Freijedo, S. Golestan, and J. M. Guerrero, "Inducverters: Pll-less converters with auto-synchronization and emulated inertia capability," *IEEE Transactions on Smart Grid*, vol. 7, no. 3, pp. 1660–1674, May 2016.

[15] G. C. Konstantopoulos, Q.-C. Zhong, and W.-L. Ming, "PLL-less nonlinear current-limiting controller for single-phase grid-tied inverters: Design, stability analysis and operation under grid faults," *IEEE Trans. Ind. Electron.*, vol. 63, no. 9, pp. 5582–5591, Sept 2016.

[16] S. Mo, B. Peng, Z. Shuai, J. Wang, C. Tu, Z. J. Shen, and W. Huang, "A new self-synchronization control strategy for grid interface inverters with local loads," in *2015 IEEE Energy Conversion Congress and Exposition (ECCE)*, Sept 2015, pp. 2316–2320.

[17] T. Midtsund, J. A. Suul, and T. Undeland, "Evaluation of current controller performance and stability for voltage source converters connected to a weak grid," in *The 2nd International Symposium on Power Electronics for Distributed Generation Systems*, June 2010, pp. 382–388.

[18] Q. C. Zhong, P. L. Nguyen, Z. Ma, and W. Sheng, "Self-synchronized synchronverters: Inverters without a dedicated synchronization unit," *IEEE Transactions on Power Electronics*, vol. 29, no. 2, pp. 617–630, Feb 2014.

[19] N. Bottrell and T. C. Green, "Comparison of current-limiting strategies during fault ride-through of inverters to prevent latch-up and wind-up," *IEEE Transactions on Power Electronics*, vol. 29, no. 7, pp. 3786–3797, July 2014.

[20] A. D. Paquette and D. M. Divan, "Virtual impedance current limiting for inverters in microgrids with synchronous generators," *IEEE Trans. Ind. Appl.*, vol. 51, no. 2, pp. 1630–1638, 2015.

[21] Q. C. Zhong and G. C. Konstantopoulos, "Current-limiting droop control of grid-connected inverters," *IEEE Transactions on Industrial Electronics*, vol. 64, no. 7, pp. 5963–5973, July 2017.

[22] G. C. Konstantopoulos, Q. C. Zhong, B. Ren, and M. Krstic, "Bounded integral control of input-to-state practically stable nonlinear systems to guarantee closed-loop stability," *IEEE Transactions on Automatic Control*, vol. 61, no. 12, pp. 4196–4202, Dec 2016.

[23] X. Hou, Y. Sun, W. Yuan, H. Han, C. Zhong, and J. M. Guerrero, "Conventional p-omega/q-v droop control in highly resistive line of low-voltage coverter-based ac microgrid," *Energies*, vol. 9(11), no. 943, 11 2016.

[24] W. F. d. Souza, M. A. Severo-Mendes, and L. A. C. Lopes, "Power sharing control strategies for a three-phase microgrid in different operating condition with droop control and damping factor investigation," *IET Renewable Power Generation*, vol. 9, no. 7, pp. 831–839, 2015.

[25] Q. C. Zhong and Y. Zeng, "Universal droop control of inverters with different types of output impedance," *IEEE Access*, vol. 4, pp. 702–712, 2016.

[26] S. Arcuri, M. Liserre, D. Ricchiuto, T. Kerekes, and F. Blaabjerg, "Stability analysis of grid inverter lcl-filter resonance in wind or photovoltaic parks," in *IECON 2011 - 37th Annual Conference of the IEEE Industrial Electronics Society*, Nov 2011, pp. 2499–2504.